

See discussions, stats, and author profiles for this publication at: <https://www.researchgate.net/publication/5442305>

Commercial Aircraft Engine Emissions Characterization of in-Use Aircraft at Hartsfield-Jackson Atlanta International Airport

ARTICLE *in* ENVIRONMENTAL SCIENCE AND TECHNOLOGY · APRIL 2008

Impact Factor: 5.33 · DOI: 10.1021/es072029+ · Source: PubMed

CITATIONS

51

READS

75

8 AUTHORS, INCLUDING:



[Scott Herndon](#)

Aerodyne Research, Inc.

239 PUBLICATIONS 4,907 CITATIONS

[SEE PROFILE](#)



[Prem Lobo](#)

Missouri University of Science and Technol...

20 PUBLICATIONS 227 CITATIONS

[SEE PROFILE](#)



[D. E. Hagen](#)

Missouri University of Science and Technol...

123 PUBLICATIONS 1,514 CITATIONS

[SEE PROFILE](#)



[Philip D. Whitefield](#)

Missouri University of Science and Technol...

90 PUBLICATIONS 1,179 CITATIONS

[SEE PROFILE](#)

Commercial Aircraft Engine Emissions Characterization of in-Use Aircraft at Hartsfield-Jackson Atlanta International Airport

SCOTT C. HERNDON,^{*†} JOHN T. JAYNE,[†]
PREM LOBO,[‡] TIMOTHY B. ONASCH,[†]
GREGG FLEMING,[§] DONALD E. HAGEN,^{‡,||}
PHILIP D. WHITEFIELD,^{‡,⊥} AND
RICHARD C. MIAKE-LYE[†]

Aerodyne Research, Inc. Billerica, Massachusetts 01821, Center of Excellence for Aerospace Particulate Emissions Reduction Center Research, University of Missouri – Rolla, Rolla, Missouri 65409, VOLPE National Transportation Systems Center, Cambridge, Massachusetts 02142, Department of Physics, University of Missouri – Rolla, Rolla, Missouri 65409, and Department of Chemistry, University of Missouri – Rolla, Rolla, Missouri 65409

Received August 14, 2007. Revised manuscript received December 21, 2007. Accepted January 14, 2008.

The emissions from in-use commercial aircraft engines have been analyzed for selected gas-phase species and particulate characteristics using continuous extractive sampling 1–2 min downwind from operational taxi- and runways at Hartsfield-Jackson Atlanta International Airport. Using the aircraft tail numbers, 376 plumes were associated with specific engine models. In general, for takeoff plumes, the measured NO_x emission index is lower (~18%) than that predicted by engine certification data corrected for ambient conditions. These results are an in-service observation of the practice of “reduced thrust takeoff”. The CO emission index observed in ground idle plumes was greater (up to 100%) than predicted by engine certification data for the 7% thrust condition. Significant differences are observed in the emissions of black carbon and particle number among different engine models/technologies. The presence of a mode at ~65 nm (mobility diameter) associated with takeoff plumes and a smaller mode at ~25 nm associated with idle plumes has been observed. An anticorrelation between particle mass loading and particle number concentration is observed.

Introduction

Aviation is a class of transportation that has had a profound impact on international relationships, global economic development, and world awareness. The majority of exhaust from operating aircraft is emitted at altitude, posing unique challenges to understanding the impacts of the emissions and their atmospheric processing (1, 2). But significant concerns regarding impacts around airports remain, and a

number of recent studies have focused on understanding the role of aviation emissions on urban air quality through the use of improved measurements at airports (3–7) and modeling the impact of emissions on surrounding regions (8–10).

The International Civil Aviation Organization (ICAO) maintains a databank of engine certification data for commercial aviation (11). The engine certification protocol specifies that emissions of CO, NO_x, and unburned hydrocarbons (UHC) be measured using standardized equipment and sampling methodology at four engine operational points at standard day operating conditions. The power points are named takeoff (100%), climb-out (85%), approach (30%), and idle (7%), where the percentage in parentheses is the fraction of rated thrust for the engine. A standardized time spent in each of these conditions is frequently referred to as a “landing, takeoff” (LTO) cycle.

The Emissions and Dispersion Modeling System (EDMS) (12) is a computer modeling tool which estimates aviation emissions based on activity and fleet composition. Though the model draws on a variety of information sources, the ICAO engine emissions databank is the principal source for aviation emissions data. EDMS can be used for either whole airport emission inventory development or predictions of perturbations in mixing ratios due to airport related emissions.

The ICAO databank tabulates emission indices in units of grams of emission per kilogram of fuel consumed. For NO_x, emitted NO (and NO₂) is reported in terms of the mass of NO₂, and UHC is reported in terms of the equivalent mass of methane. ICAO also tabulates an exhaust opacity metric called “smoke number” (SN). An interim methodology called the “first order approximation” (FOA) is underway to correlate tabulated SN measurements to a more physical mass based representation of particulate emissions until more detailed particle measurements for aircraft engines are generally available (13). The FOA version 3 includes an adjustment for volatile particles, which are not represented in the SN data set.

This paper describes measurements conducted at Hartsfield-Jackson Atlanta International Airport near Atlanta, Georgia using two mobile laboratories located downwind of active runways. The approach uses analysis of wind advected plumes from in-use commercial aircraft. A goal of the effort is the measurement of aircraft-associated emissions following the initial dilution and atmospheric processing of the plume. The majority of the sampled plumes during this measurement campaign were emitted from engines engaging in takeoff activity. Though some of the previous in-use measurements (3) have associated specific tail numbers with emissions, the focus was on idle engine emissions. The measurement effort reported in this work is significant due to the examination of takeoff plumes. This work also uses real-time particulate measurement data and sees significant differences between the particulate emission characteristics (number vs mass) between different engine models. This work reports on the analysis of over 350 wind advected plumes.

Materials and Methods

The measurements reported here follow analysis and data reduction techniques very similar to those reported in previous work (4–6). Several improvements in this general approach to exhaust characterization will be described following a description of the location. The analytical techniques employed will be discussed as an overview.

Site Description. The measurements were conducted between September 26 and 29, 2004, at Hartsfield-Jackson

* Corresponding author e-mail: herndon@ aerodyne.com.

† Aerodyne Research, Inc.

‡ Center of Excellence for Aerospace Particulate Emissions Reduction Center Research, University of Missouri – Rolla.

§ VOLPE National Transportation Systems Center.

|| Department of Physics, University of Missouri – Rolla.

⊥ Department of Chemistry, University of Missouri – Rolla.



FIGURE 1. Hartsfield International Airport: the two points marked by the red \times are the two locations used to sample the majority of the aircraft engines reported in this work. In each case wind brought diluted aircraft exhaust to the sample location.

International Airport located near Atlanta, Georgia. This airport is a hub for Delta Airlines. Delta Airlines supported this measurement campaign through financial contributions, significant logistical support, and assistance with the engine model determinations. The Hartsfield-Jackson Atlanta International Airport handles a wide range of flights including international passenger, air-freight, and domestic air traffic. It is regarded as one of the world's busiest airports both in the number of aircraft as well as the number of passengers conveyed.

A map of the airport is depicted in Figure 1. The Aerodyne Mobile Laboratory and the University of Missouri-Rolla Center of Excellence (UMRCOE) Mobile Laboratory were colocated at the points marked by the red “ \times ”. On the Sept. 26 and 27, the prevailing winds were from the north–northeast and northeast, and the measurements were conducted at the end of a runway service road located between 9L and 9R. At this site, the sampling point was located 366 m from the active runway. The primary taxiway serving most of the commercial passenger aircraft was 560 m away. A taxiway for aircraft originating from the airfreight hanger was located 80 m away. On Sept. 28 and 29, the majority of the sampling was conducted near 27R. At this site, the sampling point was located 105 m from the active runway and 216 m from the taxiway feeding the runway.

The temperature, wind data, and a qualitative account of the cloud cover for the four days of this study are provided in Supporting Information Table S1. Higher time resolution data for the wind and temperature record were used to analyze the plume encounters.

Airframe/Engine Determination. A significant limitation of the previous work done with the Aerodyne Mobile Laboratory was the inability to associate specific engine models with the discreet plumes. In the first work at JFK (4), use of the Airline Service Quality Performance (ASQP) database was able to yield only three engine/airframe combinations that allowed for a comparison of the measurement to the engine certification data (ICAO). Therefore, a priority of this study was to record specific tail numbers. The U.S. DOT/Volpe Center correlated the tail numbers with airframe/engine model data. As a result, comparison of these measurements to the ICAO engine emissions databank values was possible. In addition to Volpe's tail number/engine data, Delta Airlines was able to provide additional information to help in unambiguously identifying their specific airplanes, which represented a large fraction of the traffic at the airport.

Categorization Approach. During the data collection, as the tail numbers were being recorded, the wind directions

and speed were carefully monitored. Using time-stamped notes, the aircraft activity was recorded along the upwind vector. Using wind speed and distance estimates, plume arrival times were estimated and corroborated with the real time CO₂ measurement. This approach led to an in-field determination of aircraft activity, classified during this mission as either takeoff or idle. The output from a time-coded webcam was consulted whenever the notes were insufficient.

Analytical Instrument Package: Aerodyne. The analytical suite and capabilities of the Aerodyne Mobile Laboratory have been described previously (14, 15). During this deployment, two sampling points at the front of the vehicle were used. With the first, the gas-phase species CO, NO, NO₂, and HCHO were measured. With the second, the particulate parameters for number concentration, black carbon mass, size-resolved number concentration, and mass-based composition information were determined. CO₂ was measured on both inlets using three different instruments.

CO₂ was determined primarily using two Licor-6262 nondispersive infrared absorption instruments. A Licor-820 was used as a redundant measurement of CO₂ on the second inlet. The in-field calibration of the CO₂ instruments was accomplished using a 590 ppmv standard and “CO₂-free” N₂. The time response of each of the Licor instruments was flow rate limited. The 1/e time response was determined to be less than 0.7 s for the CO₂ instrument on the gas-phase inlet and 0.9 s for the pair of CO₂ instruments on the second inlet. The two inlets were located on the upper portion of the front of the Aerodyne Mobile Laboratory, approximately 50 cm above a typical driver and passenger seated in the front.

NO₂ and CO were measured using tunable infrared differential absorption spectroscopy (TILDAS) using pulsed quantum cascade lasers (16). The NO₂ absorption feature, at 1606.37 cm⁻¹, has been used in previous measurement campaigns (17). CO was monitored using the infrared absorption line at 2183.2 cm⁻¹. NO and HCHO were also measured using the TILDAS approach, however lead salt diode lasers were the light sources. The NO absorption doublet at 1915 cm⁻¹ was used. HCHO and HCOOH were measured at 1765 cm⁻¹. The inlet characterization and calibration system for HCHO used during this campaign is described elsewhere (18).

Particle number concentration was determined using a TSI model 3022a condensation particle counter. Saturated butanol vapor is used to grow submicron particles to sizes where they can be optically counted. At atmospheric pressure, the instrument measures particles with 99% efficiency from

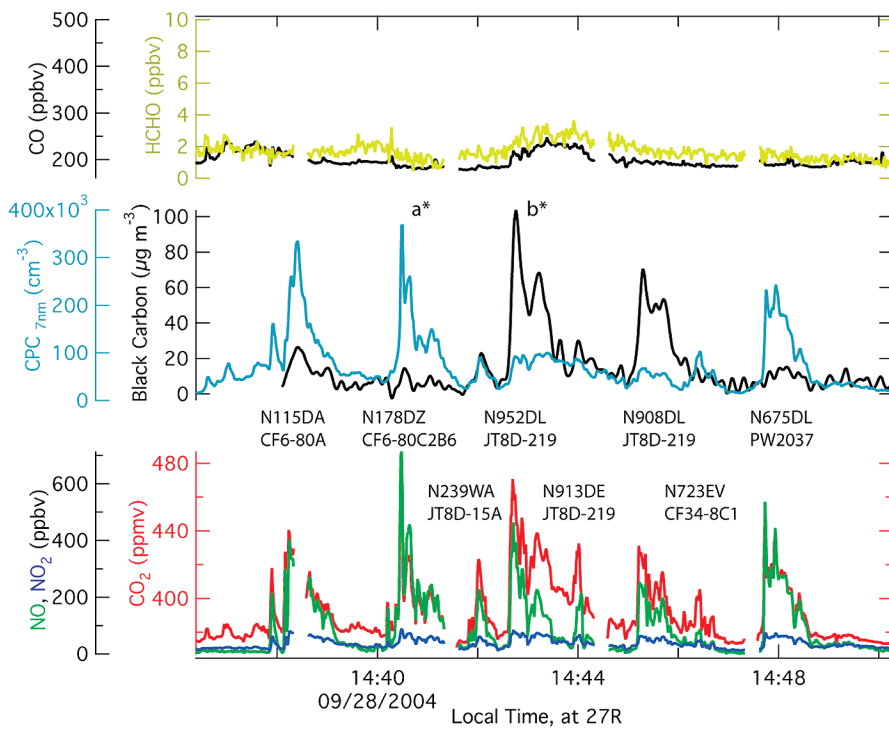


FIGURE 2. Time series of sampled data for 8 plumes. The uppermost panel depicts CO (black) and HCHO (gold). The middle panel plots the particle number concentration (light blue) and the particulate black carbon mass loading (black). In the lowest panel, the measured NO, NO_x, and CO₂ concentrations are plotted. The two CF6 engines, the CF34, and PW2037 have particulate emission characteristics very different from that of the JT8D engines after accounting for dilution using CO₂.

2.5 μm down to 20 nm, with a loss of sensitivity at smaller sizes. The specifications describe a 50% response cutoff for ~ 7 nm and the instrument essentially does not count particles below this size threshold. The upper limit of 2.5 μm was set by an inline cyclone impactor (URG Inc.). No additional corrections for sample line loss have been performed. As operated, the time response of this instrument was ~ 3 s.

Black carbon (BC) particulate mass was measured using a Thermo Electron multi-angle absorption photometer (MAAP) (19, 20). The MAAP measures particulate black carbon by collecting aerosol onto a 2 cm^2 quartz fiber filter tape. The transmission and scattering of 630 nm wavelength LED light are monitored by multiple photodetectors. A two-stream radiative transfer calculation separates the scattering from the absorption component for the total particle loading on the filter tape. The instantaneous loading is computed by the derivative of the total.

The instrument was modified for 1 s data output format and for the ability to change the sample flow rate to be selected based on the range of particle loadings encountered. This modification allowed the instrument to be used in dedicated engine tests (to be reported elsewhere) sampling concentrated exhaust immediately behind the engine, as well as the highly diluted plumes reported here, by selecting an appropriate sample flow rate. Unfortunately, since this was the first deployment of this modified instrument, the actual flow rate used for the measurements reported here was not recorded properly. Thus, while the flow through the instrument was a constant value during the study (estimated to be between 7 and 13 slpm), the absolute quantification of black carbon from this instrument as operated during this mission is uncertain, even though precise relative measurements can be reported. Due to the uncertainty in the sample flow, the absolute quantification of the black carbon loading is uncertain by some constant factor, but by the same factor for all measurements. For this reason, the emission indices for black carbon have been scaled such that the median value for the CFM-56 class of engines is 1.

Size resolved number concentration was measured using TSI scanning mobility particle sizer (SMPS) model 3080 coupled to a CPC model 3025A. The results and description of a plume compositing analysis based in this instrument are presented in the Supporting Information.

Mass-based composition data were measured using the ARI Aerosol Mass Spectrometer (AMS). The version of the AMS instrument deployed in this study used a quadrupole mass spectrometer as the mass detector. The AMS can report organic matter aerosol concentrations primarily reflecting lubricating oil and partially burnt diesel fuel adsorbed on the black carbon cores. Particle sulfate loadings are also observed in these measurements of aircraft emissions. The AMS system used in this study has been described in detail elsewhere (21, 22) and its description and results can be found in the Supporting Information.

Analytical Instrument Package: University of Missouri-Rolla. The analytical suite and capabilities of the UMRCOE Mobile Diagnostic Facility have been described previously (23). The package for the deployment described in this work consisted of a Cambustion DMS500, a state-of-the-art fast particulate spectrometer, to gather real-time size distribution information and total concentration of engine exhaust particulates; a differential mobility analyzer (DMA) (TSI model 3071), a traditional and slower instrument to measure aerosol size distributions; a TSI condensation particle counter (CPC) (TSI model 3022) to measure total number concentration; a fast response carbon dioxide (CO₂) detector, Sable Systems model CA-2A, to monitor sample dilution and establish emission factors; a deliquescence system to measure total soluble mass fraction; a hygrometer to measure the sample's water content; and a weather station to monitor the ambient conditions of temperature, relative humidity, pressure, and wind speed and direction. These were employed in a standard configuration (23) and have been used on previous jet engine emissions sampling campaigns (24–28).

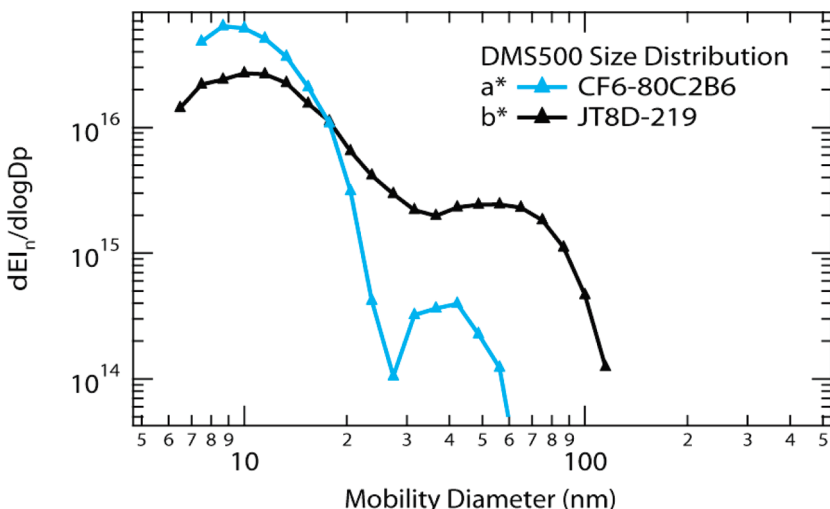


FIGURE 3. Size-resolved particle number (El_n) spectra for two plumes. The output from the DMS500 has been corrected using size-resolved measurements of the particle line transmission characteristics and the ambient background size spectrum. The CF6- and JT8D- engines measured in Figure 2 (at a* and b*) are plotted here.

Size Distribution Measurements with DMS500. The DMS500 relies upon electrical mobility for particle sizing (29). In this instrument the aerosol sample is passed through a cyclone separator to remove particles larger than $1\text{ }\mu\text{m}$ and electrically charged with a corona charger. The electrically charged particle sample is then introduced into a strong electrical field established in a classifying column. The field forces the charged particles to drift toward an array of electrometers through a sheathing gas flow created in the column. The location at which a charged particle reaches the electrometer array depends on its aerodynamic drag/charge ratio. Real-time monitoring of the electrometer outputs provided a measure of the particle size distribution. The fast size distribution measurement rate of the DMS500 (10 Hz) allows the instrument to resolve wind advected engine plumes. The majority of the results from this instrument are being prepared for a separate article on the particulate emissions but results from two plumes are presented here.

Results and Discussion

A selected time series of advected plume data from Sept. 28 is shown in Figure 2. This figure depicts several gas-phase and particulate measurements as a function of time. On the lowest panel in the figure, the CO_2 dilution fiduciary is shown to be $\sim 380\text{ ppmv}$ when the airmass being sampled contains only trace quantities of upwind exhaust (from the terminal and further upwind). The concentration of CO_2 increases rapidly ($\sim 3\text{ s}$) by plume hits of $\sim 30\text{ ppmv}$ which last for tens of seconds. Concomitant increases in the concentrations of NO and NO_2 (also shown on the lowest panel of Figure 2) are observed. The time scale of the variations in NO_x are well matched to CO_2 . The CO_2 plume strengths measured in the UMRCOE Mobile Laboratory and the Aerodyne Mobile Laboratory were similar, despite the $\sim 3\text{ m}$ separation between the sampling probes.

The middle panel of Figure 2 shows the response of the CPC number concentration and the MAAP black carbon mass loading. The four JT8D series engines have a greater black carbon mass loading than the other engines in this figure. The CF6 series engines, the CF34 and PW2037 engines have much greater particle number concentration emissions than the JT8D engines.

The size distribution spectra for the plumes marked a* and b* in Figure 2 are depicted in Figure 3. The DMS500 average size spectra for the two marked plumes are plotted. These spectra have been corrected using a sample line

transmission function determined in a calibration experiment. The description of the correction, as well as the results from the entire measurement campaign will be detailed in future work. In the context of this paper, the size distribution spectra suggest very different characteristics between the takeoff plumes of these two different engine technologies.

The emission characteristic of the JT8D indicates the presence of a soot mode between 60 and 80 nm, which is plausibly comprised of black carbon mass based on the MAAP result and previous studies (30–33). This is very different from the CF6 and PW2047 measurements, which have a greater number emission index in both the smallest diameters of the DMS500 and the CPC total number loading result. The difference between the effective particulate emissions characteristics between this engine pair more generally applies to observations throughout this measurement campaign. Typically, the particle mass loading was inversely related to particle number loading. This is consistent with previous observations (5), which showed an inverse relationship between a measurement of surface bound polyaromatic hydrocarbons and particle number concentrations. Though the comparison of surface PAH and black carbon mass is not quantitative, the observation in this study is consistent. The previous study did not attempt to record aircraft tail numbers, and as a result the finding was limited to comparing average values between different operational modes. In this work, the very robust anticorrelation is seen between different engine models operating at the takeoff condition.

The Aircraft Particulate Emissions eXperiment (APEX-1) study (34) indicates the particulate mass is essentially a conserved quantity as the plume dilutes downwind, while the particle number observed in the CFM-56 (and presumably for the CF6-, CF34-, and PW2037 in Figure 2) is a consequence of post emission condensation. This is corroborated by the SMPS analysis discussed in the Supporting Information. Though the SMPS is significantly slower than the DMS500, it can be used to determine the composite mobility diameter mode sizes using the gas-phase determination of plume origin.

In the ICAO engine emissions databank, the CO and NO_x emission indices are inversely related. This is due primarily to incomplete combustion at lower combustor temperatures leading to the production of CO. As the combustor temperature increases, the CO emissions are minimized but the NO_x emission index increases. This relationship is observed in Figure 4. The individual plume emission indices for CO

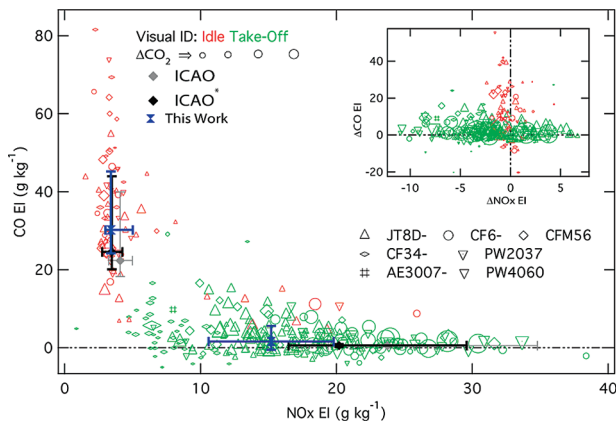


FIGURE 4. CO vs NO_x emission indices. The measured CO emission indices are plotted vs the NO_x emission indices. The colors of the data points reflect the visual identification of the plume origin: idle (red), takeoff (green). The size of the data point indicates the strength of the plume hit reflected in the CO₂ concentration. The symbols are the tabulated ICAO, BFFM2 corrected ICAO, and bulk categorical averages measured in this work. The inset depicts the plume by plume difference between the measured and corresponding ICAO predicted value. See text for additional discussion.

have been plotted vs NO_x emission indices. This sample includes the data collected on Sept. 27 and 29. The visual identification of the aircraft activity (idle or takeoff) splits the data into the two groups seen in Figure 4. The black diamonds are the ICAO engine emissions databank data that have been corrected using the Boeing Fuel Flow Method 2 (35). Using the ASQP and notes records, average CO and NO_x emission indices for takeoff and idle were computed, weighted by the frequency of each specific engine in use at Hartsfield-Jackson from Sept. 26 to 29. The 25th and 75th quartiles of this population are shown as error bars to convey a sense of the expected distribution. The population of engine types sampled during this study includes a wide range of engine types and the comparison of median in-use to median ICAO population has been done to get a sense of the qualitative level of agreement. The calculated emission indices for both gas-phase compounds and particulate loadings are summarized in Table 1.

CO and NO_x at Idle. The data in Figure 4 indicate the measured CO emission index is greater than the predicted emission index by almost 50% (blue vs black). The measured CO emission index ranges from 17.6 to 39.2 g kg⁻¹ (25th and 75th quartiles respectively) in the total population of sampled idle plumes (82). The median value for all idle plumes is tabulated in Table 1. The engines measured in this real world context were not being run at the 7% of rated thrust, which ICAO convention uses as the “idle” condition for certification measurements. As a result, this is not an unexpected observation. Furthermore, it should not necessarily be interpreted that total emissions of CO are under-represented in inventories based on the difference observed here. Total emissions burdens are the product of the fuel flow rate, emission index, and time spent in the actual operational mode. The fuel flow rate during routine operational idle is less than the tabulated 7% fuel flow rate. The impact of these competing factors on emission inventory will be the subject of future work.

The NO_x emission index average for idle emissions is 15% lower than the ICAO prediction (blue vs black in Figure 4). Fuel flow rate is also lower for the routine operational idle. In this case, as both contributing factors point in the same direction, these results suggest that the NO_x total emissions burden resulting from the time spent at idle would be overrepresented in inventories developed using 7% certification emission indices.

NO_x at Takeoff. The NO_x emission indices measured in this work range from 10.7 to 22 g kg⁻¹ (25th and 75th quartiles) in the 294 plumes identified as originating from takeoff activity. The median value is tabulated in Table 1. Each measured plume has been compared to the specific predicted value using engine emission certification data. The average difference between the measured and predicted emissions indices suggests the engine certification data predictions overestimate NO_x emissions by ~18%. A very likely reason for this result is the practice of reduced thrust takeoff (36). When the total cargo, passenger weight, and fuel load are below the takeoff weight rating for the aircraft and ambient conditions allow, at the pilot’s discretion, a thrust less than the maximum rated thrust can be used to effect the takeoff. This practice helps prolong the time between engine maintenance scheduling.

TABLE 1. Summary of September 27 and 29 Results

	n	NO _x E (g kg ⁻¹)	ΔNO _x ^a	CO EI (g kg ⁻¹)	ΔCO ^a	HCHO EI (g kg ⁻¹)	CPC Eln (# kg ⁻¹)	BC ^c	ICAO SN ^b
take-off									
CF34	45	7.2	-2.7	2.9	2.5	0.15	3.7E+15	1.5	11.1
JT8D	84	15.0	-0.5	2.0	1.6	0.10	1.8E+15	3.0	14.3
CFM56	27	15.4	-3.4	1.7	1.3	0.13	5.6E+15	1.0 ^c	7.9
PW2037	24	21.1	-4.4	1.5	1.1	0.10	3.6E+15	1.0	na
CF6	37	22.0	-3.5	1.0	0.6	0.07	4.6E+15	0.8	7.3
all engines	294	15.3	-2.8	1.6	1.1	0.11	3.2E+15	1.6	
idle									
CF34	13	3.4	0.0	44.0	4.6	0.74	5.5E+15	0.9	na
JT8D	24	4.0	-0.1	27.0	14.0	0.72	4.5E+15	1.1	na
CFM56	10	3.3	-0.7	48.0	23.0	1.09	8.2E+15	0.3	2.1
PW2037	9	3.9	-0.3	28.7	8.5	0.75	4.5E+15	0.6	na
CF6	9	3.7	0.4	34.0	11.0	0.69	4.0E+15	0.6	1.4
all engines	82	3.8	-0.5	29.0	14.0	1.01	5.7E+15	0.8	

^a The difference between the measured NO_x or CO EI and the ICAO tabulated EI was computed for each specific engine model, i.e. tabulated values for the “JT8D-219” when that was the appropriate data to use. ^b When computing the difference, the specific ICAO value was adjusted using the Boeing Fuel Flow Method 2 (described in the text) for the meteorological conditions at the time of the measurement. ^c As described in the Materials and Methods section, the black carbon data measured using the MAAP have been scaled to the median value for takeoff for the CFM56 results, which has been assigned a value of 1.

HCHO Emission Indices. HCHO emission indices were measured. This work represents the first time the HCHO and CO emissions were measured simultaneously in wind advected plumes. A typical ratio observed between these species is 21 ± 8 pptv ppbv⁻¹ for plumes identified as “idle”, where the uncertainty is one standard deviation in the distribution of plume ratios. The HCHO emission index determined in this work for different engines agrees well with the range of values encountered in previous studies (6). It is known that emissions of hydrocarbon species vary greatly with temperature and small changes in the near-idle throttle level (37, 38). The engine certification value, UHC, does not directly relate to equivalent HCHO. The implications of the emissions of HCHO will be subject of future work investigating initial chemistry in the diluting plume.

Total Particle Number Emission Index. The median value of the particle number emission index (EI_n) is compiled in Table 1. Qualitatively, the idle plumes have a greater particle number emission index than the takeoff plumes. This phenomenon has been observed previously in plumes encountered in flight (39, 40), in staged engine testing (33), and at airports (5). Similar to previous observations, the distribution of observed EI_n is broad ($\pm 50\%$ of the median value). A qualitative anticorrelation between particle number and black carbon mass is also present in the tabulated values. This phenomenon is likely being driven by two considerations. The first is that typically, the black carbon emission index is greater at higher power, providing greater surface area which promotes condensation of non- and semivolatile species and inhibits growth of nucleation mode particles. The second influence involves the amount of condensable organic mass. At idle, the HCHO and CO emission indices are an order of magnitude larger than at takeoff. These gas-phase species are good proxies for the degree of combustion inefficiency. It is plausible that the mass of partially oxidized hydrocarbons with lowered volatility is greater in the idle plumes than at takeoff. The assimilation of these results together with measurements at other airports in a particle microphysics model is ongoing.

Black Carbon Emission Index. The median value of a normalized black carbon emission index for the classes of engines sampled in this work is included in Table 1.

Based on the estimate of the flow rate, the value of 1 corresponds to an absolute mass loading of 270–501 mg kg⁻¹ fuel. This is somewhat greater than the black carbon emission index determined for the CFM56-2C1 (~ 200 –250 mg kg⁻¹) during APEX-1 (33). One explanation involves differences in the specific engine model in APEX-1 and the population in this sample. The best proxy in the ICAO databank for the CFM56-2C1 has a smoke number of 6 while the median smoke number in this population is slightly greater (7.9). More recent APEX campaigns (2 and 3) expand the number of specific CFM56 tested and should shed light on the difference observed here.

Acknowledgments

We gratefully acknowledge the financial support of NASA (Chowen Wey, project monitor) and FAA for PARTNER Project 9 (Carl Ma, project monitor), both through the University of Missouri, Rolla’s Center of Excellence for Aerospace Particulate Emissions Reduction, directed by P.D. Whitefield. Extensive logistical support and in-kind time and effort were provided by the Hartsfield-Jackson Atlanta International Airport by T. Nissalke and colleagues. Delta Airlines (Jim Brooks) provided valuable support. We thank Robert Prescott for his tireless effort in logistic support.

Supporting Information Available

Two of the key particulate measurement results discussed in this paper: the SMPS measured idle/takeoff differences and the AMS measured sulfate size distributions (Figures

SI-1 and SI-2, respectively); a detailed list of the various meteorological conditions during this measurement effort (Table S1). This material is available free of charge via the Internet at <http://pubs.acs.org>.

Literature Cited

- (1) IPCC, Ed. *Aviation and the Global Atmosphere*; Cambridge University Press: Cambridge, U.K., 1999.
- (2) Rogers, H. L.; Lee, D. S.; Raper, D. W.; Foster, P. M. d. F.; Wilson, C. W.; Newton, P. J. The impact of aviation on the atmosphere. *Aeronautical J.* **2002**, *106*, 521–546.
- (3) Schäfer, K.; Jahn, C.; Sturm, P.; Lechner, B.; Bacher, M. Aircraft emission measurements by remote sensing methodologies at airports. *Atmos. Environ.* **2003**, *37*, 5261–5271.
- (4) Herndon, S. C.; Shorter, J. H.; Zahniser, M. S.; Nelson, D. D., Jr.; Jayne, J.; Brown, R. C.; Miake-Lye, R. C.; Waitz, I.; Silva, P.; Lanni, T.; Demerjian, K.; Kolb, C. E. NO and NO₂ Emissions Ratios Measured from in-use Commercial Aircraft during Taxi and Take-Off. *Environ. Sci. Technol.* **2004**, *38*, 6078–6084.
- (5) Herndon, S. C.; Onasch, T. B.; Frank, B. P.; Marr, L. C.; Jayne, J. T.; Canagaratna, M. R.; Grygas, J.; Lanni, T.; Anderson, B. E.; Worsnop, D. R.; Miake-Lye, R. C. Particulate emissions from in-use commercial aircraft. *Aerosol Sci. Technol.* **2005**, *39*, 799–809.
- (6) Herndon, S. C.; Rogers, T.; Dunlea, E. J.; Miake-Lye, R. C.; Knighton, B. Hydrocarbon emissions from in-use commercial aircraft during airport operations. *Environ. Sci. Technol.* **2006**, *40*, 4406–4413.
- (7) Schürmann, G.; Schäfer, K.; Jahn, C.; Hoffmann, H.; Bauerfeind, M.; Fleuti, E.; Rappenglück, B. The impact of NO_x, CO and VOC emissions in the air quality of Zurich Airport. *Atmos. Environ.* **2007**, *41*, 103–118.
- (8) Pison, I.; Menut, L. Quantification of the impact of aircraft traffic emissions on tropospheric ozone over Paris area. *Atmos. Environ.* **2004**, *38*, 971–983.
- (9) Yu, K. N.; Cheung, Y. P.; Chueng, T.; Henry, R. C. Identifying the impact of large urban airports on local air quality by nonparametric regression. *Atmos. Environ.* **2004**, *38*, 4501–4507.
- (10) Unal, A.; Hu, Y.; Chang, M. E.; Odman, M. T.; Russel, A. G. Airport related emissions and impacts on air quality: Application to the Atlanta international Airport. *Atmos. Environ.* **2005**, *39*, 5787–5798.
- (11) ICAO. International Civil Aviation Organization Aircraft Engine Emissions Databank; <http://www.caa.co.uk/docs/702/introduction-05102004.pdf>; 2006.
- (12) Anderson, C.; Augustine, S.; Embt, D.; Thrasher, T.; Plante, J. *Emissions and Dispersion Modeling System (EDMS) User’s Manual*; AAE-07-01, Revision 3; Federal Aviation Administration, Office of Environment and Energy: Washington, DC, 2007.
- (13) Wayson, R.; Fleming, G. G.; Kim, B.; Draper, J. Derivation of a First Order Approximation of Particulate Matter from Aircraft, www.volpe.dot.gov/air/docs/69970.pdf; 2006, pp 1–9.
- (14) Herndon, S. C.; Jayne, J. T.; Zahniser, M. S.; Worsnop, D. R.; Knighton, B.; Alwine, E.; Lamb, B. K.; Zavala, M.; Nelson, D. D.; McManus, J. B.; Shorter, J. H.; Canagaratna, M. R.; Onasch, T. B.; Kolb, C. E. Characterization of urban pollutant emission fluxes and ambient concentration distributions using a mobile laboratory with rapid response instrumentation. *Faraday Discuss.* **2005**, *130*, 327–339.
- (15) Kolb, C. E.; Herndon, S. C.; McManus, J. B.; Shorter, J. H.; Zahniser, M. S.; Nelson, D. D.; Jayne, J. T.; Canagaratna, M. R.; Worsnop, D. R. Mobile Laboratory with Rapid Response Instruments for Real-time Measurements of Urban and Regional Trace Gas and Particulate Distributions and Emission Source Characteristics. *Environ. Sci. Technol.* **2004**, *38*, 5694–5703.
- (16) Jimenez, R.; Herndon, S. C.; Shorter, J. H.; Nelson, D. D., Jr.; McManus, J. B.; Zahniser, M. Atmospheric trace gas measurements using a dual quantum-cascade laser mid-infrared absorption spectrometer. *SPIE Proc.* **2005**, *5738*, 318.
- (17) Shorter, J. H.; Herndon, S. C.; Zahniser, M. S.; Nelson, D. D., Jr.; Wormhoudt, J.; Demerjian, K. L.; Kolb, C. E. Real-time Measurements of Nitrogen Oxide Emissions from In-use New York City Transit Buses using a Chase Vehicle. *Environ. Sci. Technol.* **2005**, *39*, 7991–8000.
- (18) Herndon, S. C.; Zahniser, M. S.; Nelson, D. D.; Shorter, J. H.; McManus, J. B.; Jimenez, R.; Warneke, C.; de Gouw, J. A. Airborne measurements of HCHO and HCOOH during the New England Air Quality Study 2004 using a pulsed quantum cascade laser spectrometer. *J. Geophys. Res.* **2007**, *112*, D10S03.

- (19) Petzold, A.; Schonlinner, M. Mult-angle absorption photometry—a new method for the measurement of aerosol light absorption and atmospheric black carbon. *J. Aerosol Sci.* **2004**, *35*, 421–441.
- (20) Petzold, A.; Schloesser, H.; Sheridan, P. J.; Arnott, W. P.; Ogren, J. A.; Virkkula, A. Evaluation of Multi-Angle Absorption Photometry for Measuring Aerosol Light Absorption. *Aerosol Sci. Technol.* **2005**, *39*, 40–51.
- (21) Jayne, J. T.; Leard, D. C.; Zhang, X.; Davidovits, P.; Smith, K. A.; Kolb, C. E.; Worsnop, D. R. Development of an Aerosol Mass Spectrometer for Size and Composition Analysis of Submicron Particles. *Aerosol Sci. Technol.* **2000**, *33*, 49–70.
- (22) Canagaratna, M. R.; Jayne, J. T.; Ghertner, D. A.; Herndon, S.; Shi, Q.; Jiménez, J. L.; Silva, P.; Williams, P.; Lanni, T.; Drewnick, F.; Demerjian, K. L.; Kolb, C. E.; Worsnop, D. R. Chase Studies of Particulate Emissions from in-use New York City Vehicles. *Aerosol Sci. Technol.* **2004**, *38*, 555–573.
- (23) Schmid, O.; Hagen, D. E.; Whitefield, P. D.; Trueblood, M. B.; Rutter, A. P.; Lilenfeld, H. V. Methodology for Particle Characterization in the Exhaust Flows of Gas Turbine Engines. *Aerosol Sci. Technol.* **2004**, *38*, 1108–1122.
- (24) Hagen, D. E.; Paladino, J.; Whitefield, P. D.; Trueblood, M. B.; Lilenfeld, H. V. Airborne and ground based jet engine aerosol emissions sampling during two NASA field projects: SUCCESS and SNIF. *J. Aerosol Sci.* **1997**, *28*, S67–S68.
- (25) Hagen, D. E.; Whitefield, P. D.; Paladino, J.; Trueblood, M. B.; Lilenfeld, H. V. Particulate sizing and emission indices for a jet engine exhaust sampled at cruise. *Geophys. Res. Lett.* **1998**, *25*, 1681–1684.
- (26) Hagen, D. E.; Whitefield, P. D.; Paladino, J.; Schmid, O.; Schlager, H.; Schulte, P. Atmospheric aerosol measurements in the North Atlantic flight corridor during project POLINAT-2. *J. Aerosol Sci.* **1999**, *30*, 161–162.
- (27) Whitefield, P. D.; Ross, M.; Hagen, D. E.; Hopkins, A. Aerosol characterization in rocket plumes. *J. Aerosol Sci.* **1999**, *30*, 215–216.
- (28) Lobo, P.; Hagen, D. E.; Whitefield, P. D.; Alofs, D. J. Physical characterization of aerosol emission from a Commercial Gas Turbine Engine. *J. Propulsion Power* **2007**, *23*, 919–929.
- (29) Biskos, G.; Reavell, K.; Collings, N. Description and Theoretical Analysis of a Differential Mobility Spectrometer. *Aerosol Sci. Technol.* **2005**, *39*, 527–541.
- (30) Anderson, B. E.; Cofer, W. R.; Bagwell, D. R.; Barrick, J. D.; Hudgins, C. H.; Brunke, K. E. Airborne observations of aircraft aerosol emissions I: Total nonvolatile particle emission indices. *Geophys. Res. Lett.* **1998**, *25*, 1689–1692.
- (31) Anderson, B. E.; Winstead, E.; Hudgins, C. H.; Plant, J.; Branham, H. S.; Thornhill, L.; Boudries, H.; Canagaratna, M. R.; Miake-Lye, R. C.; Wormhoudt, J.; Worsnop, D. R.; Miller, T.; Ballenthin, J.; Hunton, D.; Viggiano, A.; Pui, D. Y. H.; Han, H. S.; Blake, D.; McEachern, M. Overview of results from the NASA experiment to characterize aircraft volatile aerosol and trace species emissions (EXCAVATE). *Proc. Atm. Avia. and Climate* 2003, Friedrichschafen, Germany.
- (32) Anderson, B. E.; Winstead, E. L.; Hudgins, C. H.; Thornhill, K. L. *Concentrations and Physical Properties of Particles Within the Exhaust of a CFM-56 Engine*; NASA/TM-2006-214382; ARL-TR-3903, Appendix H; NASA: Washington, DC, 2006.
- (33) Wey, C. C.; Anderson, B. E.; Wey, C.; Miake-Lye, R. C.; Whitefield, P. D.; Howard, R. Overview of the Aircraft Particle Emissions Experiment. *J. Propulsion Power* **2007**, *23*, 898–905.
- (34) Wey, C. C.; Anderson, B. E. *Aircraft Particle Emissions eXperiment (APEX)*; NASA/TM-2006-214382; ARL-TR-3903; NASA: Washington, DC, 2006.
- (35) DuBois, D.; Paynter, G. C. “Fuel Flow Method2” for Estimating Aircraft Emissions; 2006-01-1987; SAE Technical Paper Series; Society of Automotive Engineers: Warrendale, PA, 2006.
- (36) FAA. *Reduced and Derated Takeoff Thrust (Power) Procedures*; Advisory Circular AC 25-13; 1988.
- (37) Yelvington, P. E.; Herndon, S. C.; Wormhoudt, J. C.; Jayne, J. T.; Miake-Lye, R. C.; Knighton, W. B.; Wey, C. C. Chemical Speciation of Hydrocarbon Emissions from a Commercial Aircraft Engine. *J. Propulsion Power* **2007**, *23*, 912–918.
- (38) Knighton, W. B.; Rogers, T.; Wey, C. C.; Anderson, B. E.; Herndon, S. C.; Yelvington, P. E.; Miake-Lye, R. C. Application of Proton Transfer Reaction Mass Spectrometry (PTR-MS) for Measurement of Volatile Organic Trace Gas Emissions From Aircraft. *J. Propulsion Power* **2007**, *23*, 949–958.
- (39) Anderson, B. E.; Cofer, W. R.; Barrick, J. D.; Bagwell, D. R.; Hudgins, C. H. Airborne observations of aircraft aerosol emissions II: Factors controlling volatile particle production. *Geophys. Res. Lett.* **1998**, *25*, 1693–1696.
- (40) Schröder, F. P.; Brock, C. A.; Baumann, R.; Petzold, A.; Busen, R.; Schulte, P.; Fiebig, M. In situ studies on volatile jet exhaust particle emissions: Impact of fuel sulfur content and environmental conditions on nuclei mode aerosols. *J. Geophys. Res.* **2000**, *105*, 19941–19954.

ES072029+